Support Conditions for Experimental Modal Analysis

Thomas G. Carne, **D. Todd Griffith** and **Miguel E. Casias**
Sandia National Laboratories, Albuquerque, New Mexico

When modal testing a structure for model validation, free boundary conditions are frequently approximated in the lab to compare with free boundary-condition analyses. Free conditions are used because they are normally easy to simulate analytically and easier to approximate experimentally than boundary conditions with fixed conditions. However, the free conditions can only be approximated in the lab, because the structure must be supported in some manner. This article investigates and quantifies the effects of the support conditions on both the measured modal frequencies and damping factors. The investigation has determined that the measured modal damping is significantly more sensitive to the support system (stiffness and damping) than the measured modal frequency. Included in the article are simple formulas that can be used to predict the effect on measured modal parameters given the support stiffness and damping.

Modal testing is frequently used to validate the accuracy of structural dynamic models. Modal tests are performed on a structure to measure the modal frequencies, damping factors, and mode shapes. However during the modal test, a structure must be supported in some manner by the surrounding environment. Very frequently, free boundary conditions are the desired support conditions for comparison with computational results. Free conditions can only be approximated in the lab using soft supports, but the stiffness and damping of these added supports will affect the modal parameters of the combined structural system. A required part of pre-test planning is to design the support system to minimally affect the modal parameters. Obviously, one can include a model of the support system as part of the overall system model, and sometimes that is required due to compromises involved in the support system design. But one would like to be able to calculate the effects of the support system on the modal parameters to determine whether the effects are negligible or need to be accounted for.

One of the primary objectives of this article is to derive fairly simple formulas and rules of thumb by which one can calculate the effect of the support conditions on the measured modal frequencies and damping factors so that appropriate support design can be performed before the test. The formulas and the effects of poor support conditions are also illustrated with results from two different modal tests.

Historically, there has been concern for support stiffness and its effect on measured modal frequencies. Bisplinghoff, Ashley and Halfman[1] discuss the effects of support stiffness and mass on the modal frequencies, based on results of Rayleigh.[2] Wolf[3] discusses the effects of support stiffness with regard to modal testing of automotive bodies. He reports that the rule of thumb to simulate free boundary conditions is to design the support system so that the rigid-body modes, that is, the modes that would be at zero frequency except for the support conditions, are no more than one-tenth the frequency of the lowest elastic mode. But it is seldom possible to achieve this separation for vehicle tests. He states that test engineers frequently use a 1:3 to 1:5 separation ratio between the rigid-body modes and the lowest elastic mode. Wolf shows that such stiff supports can lead to significant errors in the measured

Figure 1. Freely supported two DOF system.
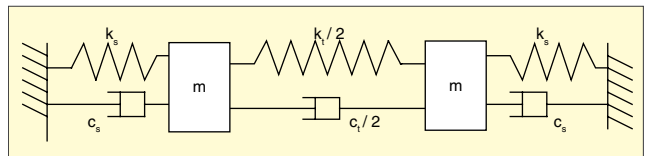
Figure 2. Two DOF system with added support stiffness and damping.

modal frequencies. One of the current authors discussed support conditions in an earlier work,[4] and this article expands on that work with additional theoretical results and illustrates the theory with experiments and modeling. In his second edition of *Modal Testing*,[5] Ewins briefly discusses the issue of location of suspensions for free boundary conditions in the test planning chapter. More recently, Brillhart and Hunt presented an exposition of many of the practical difficulties involved in designing good fixtures for a modal test,[6] and Avitabile briefly discussed this issue in a "Back to Basics" article.[7]

In this article our primary emphasis here was to develop some quantitative measures of the effect of the support conditions on the modal frequencies and the modal damping ratios. Most finite-element models could include the support stiffnesses and masses in the model, thus taking into account those effects. However, structural dynamic models often do not initially include damping, but use the measured modal damping ratios from a test to create a model, including damping. There is typically no validation of the damping model; it is taken directly from the test with the support conditions included. Consequently, one must be concerned with how the support conditions affect the measured damping. The remainder of this article is divided into four primary sections. In the first section, simple formulas are derived for a two degree-of-freedom system. These formulas are simplistic, but can be used to derive rules of thumb and also easily illustrate the severity of the problem. The next section develops approximate formulas for the multi-degree-of-freedom problem that can be used for general structures. The last two sections further illustrate both the problem and the theory with some example modal tests, first from a very lightly damped uniform beam and second with a wind turbine blade that required a modal test for model validation and damping determination.

The Two Degree-of-Freedom System

Perhaps the best way to develop an understanding of the effects of support conditions is to examine a two degree-of-freedom (DOF) system. Wolf[3] also analyzed a two DOF system, but we examine a somewhat different system that also includes damping. Let us consider a simple model, pictured in Figure 1, of an unconstrained structure (free boundary conditions), consisting of two masses connected by a linear spring and a viscous damper with motion restricted to a single direction.

We could add support conditions in several ways, but let us add them symmetrically as diagrammed in Figure 2. In these figures, the *t* subscript designates parameters for the true system, while the *s* subscript designates the added support stiffness and damping. One

could write down the equations of motions for this simple system, but using the symmetry, the modal parameters can be solved by inspection. There are two modes for this system $\phi_1 = [1\ 1]^T$ and $\phi_2 = [1\ -1]^T$. The first mode is referred to as the support mode or the rigid-body mode, because there is no deformation in the original structure (Figure 1). The second mode is the elastic mode, because it involves elastic deformation of the original structure. The undamped natural frequencies for the two modes are:

$$\omega_s = \sqrt{k_s/m} \qquad \omega_m = \sqrt{(k_t + k_s)/m} \qquad (1)$$

where ω_s indicates the mode due to the support system while ω_m indicates the mode of the measured system including the support. Similarly, the damping factors can be derived from inspection and are:

$$\zeta_s = c_s/2m\omega_s \qquad \zeta_m = (c_s + c_t)/2m\omega_m \qquad (2)$$

Following Wolf's example,[3] we now define symbols for the true natural frequency and damping factor of the structure if it had no supports as:

$$\omega_t = \sqrt{k_t/m} \qquad (3a)$$

$$\zeta_t = c_t/2m\omega_t \qquad (3b)$$

Combining Equations 1 and 3a, we find a very simple and easily remembered expression relating the measured frequency ω_m to the true frequency ω_t and the support frequency ω_s:

$$\omega_m^2 = \omega_t^2 + \omega_s^2 \qquad (4)$$

Or the true frequency can be expressed as:

$$\omega_t = \omega_m\left[1 - \frac{\omega_s^2}{\omega_m^2}\right]^{1/2} \qquad (5)$$

And if $\omega_s/\omega_m \ll 1.0$, then:

$$\frac{\Delta\omega}{\omega_m} = \frac{\omega_m - \omega_t}{\omega_m} \cong \frac{1}{2}\left(\frac{\omega_s}{\omega_m}\right)^2 \qquad (6)$$

From Equation 6, it is easy to see the effect of added support stiffness on the measured frequency of the test item. If the support stiffness is such that the ratio of the rigid-body frequency ω_s to the measured frequency ω_m is 1:10; then the true frequency would be approximately one half of 1 percent different from the measured frequency. So the 1:10 ratio is a good rule of thumb for most applications for reasonable accuracy. However, if the ratio were 1:3 as discussed by Wolf, then the error would be over 5 percent, which generally would be unacceptable. Wolf shows a case where the error would be even as large as 15 percent for a different dynamic system. Wolf's example illustrates where this simple rule of thumb, Equation 5, is just that, a very simplistic approximation. For example, envision supporting a horizontal beam with two vertical, soft bungee cords and wanting to measure the first bending mode of the beam. If the supports are attached at the extreme ends of the beam, then the supports would have a much greater effect on that modal frequency. In fact, the effect would be four times greater than that shown in Equation 5. One would need to insert the multiplier of 4.0 in front of the ω_s term. In contrast, if the supports are attached at the node points of the bending mode, then the supports would have zero effect on that particular modal frequency.

Let us now turn our attention to the measured damping ratio. Following the example of the frequency analysis above, combining Equations 2 and 3b, we find another simple formula relating the damping factors:

$$\zeta_m\omega_m = \zeta_t\omega_t + \zeta_s\omega_s \qquad (7)$$

The above expression can now be solved for the true damping ratio in terms of the measured and rigid-body damping ratios:

$$\zeta_t = \zeta_m\frac{\omega_m}{\omega_t}\left[1 - \frac{\omega_s}{\omega_m}\frac{\zeta_s}{\zeta_m}\right] \qquad (8)$$

This expression is similar to Equation 5 (frequencies), except that the frequency ratio inside the brackets is no longer squared, and it is also multiplied by the ratio of the damping ratios. So if we have a frequency ratio of 1:10, as the rule of thumb suggests, and

if the support and measured damping ratios ζ_s and ζ_m are equal; then there would be a 10 percent error if the true damping was assumed equal to the measured damping.

However, suppose now we are testing a moderately damped structure, the frequency ratio is still 1:10, but the support damping is 5 percent and the measured damping is 1 percent. Now the ratio of dampings in the bracket is 5.0 and has a large effect. The true damping would only be 0.5 percent, so one would have a 100 percent error if one assumed the measured damping was the true damping. Lastly, let us now consider the case where the frequency ratio is 1:3. If the true damping ratio is again 0.5 percent and the support damping ratio is 5 percent, then the measured damping ratio would be 2.59 percent, resulting in 400 percent error if one assumed the measured damping was the true damping.

From these examples and Equation 7, the situation for the measured damping ratios is different from that for the measured modal frequencies. An assumption that the true damping ratio is the same as the measured damping ratio can result in huge errors as compared to those for the modal frequencies. Unfortunately, many finite-element models do not include damping, and frequently, test-derived modal damping is used in the model to create the damping model.

Now, there is one saving factor in measuring modal damping. The viscous damping model (one that is independent of frequency) is frequently not a good model for many support structures, including bungee cords and airbags. Damping in materials and the estimation of damping models has been the subject of many papers, just a few have been referenced here,[8-11] since examining damping models is beyond the scope of this work. But many authors would use a structural or solid damping model, at least in part, to model damping. Using structural damping, the damping force in the differential equation is modeled by an imaginary structural damping coefficient γ times the stiffness times the displacement, rather than the viscous damping coefficient c times the velocity. So the damping force is $\sqrt{-1}\gamma k$ times the displacement, rather than c times the velocity. Using the structural damping model, then the typically measured viscous damping factor ζ at the resonant frequency is approximately equal to $\gamma/2$.[12] And Equation 7, which relates the viscous damping factors, would be modified if structural damping models are used instead of viscous damping models. The measured structural damping coefficient γ_m can be expressed as a weighted sum of the support damping γ_s and the true damping γ_t as:

$$\gamma_m = \frac{k_s\gamma_s + k_t\gamma_t}{k_t + k_s} \qquad (9)$$

Note that structural damping elements do not add in the same way as viscous damping elements. Dividing the numerator and denominator of the fraction in Equation 9 by the mass, we obtain a relationship similar in form to Equation 7 but significantly different due to the squares of the frequencies:

$$\omega_m^2\gamma_m = \omega_s^2\gamma_s + \omega_t^2\gamma_t \qquad (10)$$

This expression can be solved for the true structural damping in terms of the measured and support damping coefficients:

$$\gamma_t = \gamma_m\frac{\omega_m^2}{\omega_t^2}\left[1 - \frac{\omega_s^2}{\omega_m^2}\frac{\gamma_s}{\gamma_m}\right] \qquad (11)$$

This equation is much more forgiving of the support system damping than Equation 8, due to the squares of the frequency ratio. Also, recall that the viscous damping factor ζ at the resonant frequency is approximately equal to $\gamma/2$.[12] For example, suppose we are again testing a moderately damped structure and the frequency ratio is still 1:10, but the structural support damping is five times that of the structural measured damping, then the measured damping would contain only a 5 percent error as compared to the true damping. In the extreme case, when the frequency ratio is 1:3 and the support damping is five times that of the measured structure, then the measured damping is 50 percent in error and would be unacceptable but not nearly as bad as the viscous damping model. Even for this structural damping

model, one can still vastly overestimate the modal damping in a structure if the true damping is exceptionally small, as we will see later in this article. So, for applications with low damping, one must be particularly attentive to the added support damping regardless of the model.

The Multi-Degree-of-Freedom System

In this section, the multi-DOF problem will be examined to derive formulas similar to those above. Typically, we are only concerned with the lowest mode of the dynamic system, because it will be most affected by the support system. So one might think that the single DOF model should be sufficient, and that is frequently true. However with a multi-DOF system, the placement of the supports relative to the mode shape can be included. That is a very important aspect of the support problem. We alluded to this aspect somewhat in the previous section by mentioning that, for a beam, the frequency shift depended whether the supports were attached at the beam ends or the nodes of the first mode. If the supports were attached at the beam extremities, the effect of the support conditions was four times that which the single DOF formulas provided; and if attached at the nodes of the mode, then the effects reduced to zero.

Let us first examine the real eigenvalue problem for the multi-DOF system that yields the eigen or modal frequencies and compute the change in a particular modal frequency ω_p due to a small change in the stiffness matrix K:

$$\left[K - \omega_p^2 M \right] \phi_p = 0 \tag{12}$$

The easiest procedure is to take the partial derivative of Equation 12 with respect to just one support stiffness, say k_{ii}. This would be on the diagonal of the matrix, because the support stiffness is to ground. Using established formulas for the derivative, (see for example Ref. 5, page 152, Equation 2.165), after a few simplifications, we find:

$$\frac{\partial \omega_p}{\partial k_{ii}} = \frac{1}{2\omega_p} \phi_p^T \frac{\partial K}{\partial k_{ii}} \phi_p \tag{13}$$

Equation 13 assumes we have mass normalized modes. Now, we can let the stiffness matrix for this system be equal to the true stiffness K_t plus the support stiffness K_s, where the k_{ii} parameter only appears in the K_s matrix. Then the partial derivative of K with respect to k_{ii} would just be a matrix with all zeros, except at position i on the diagonal, where it would be unity. Using this in Equation 13, we find:

$$\frac{\partial \omega_p}{\partial k_{ii}} = \frac{1}{2\omega_p} \phi_p^i \phi_p^i \tag{14}$$

where the superscript i indicates the ith component of the vector. With this relationship for the partial derivative, we can now approximate the change in modal frequency due to the addition of a support stiffness Δk_{ii} by:

$$\frac{\Delta \omega_p}{\omega_p} \cong \frac{1}{2\omega_p^2} \left(\phi_p^i \right)^2 \Delta k_{ii} \tag{15}$$

This formula for the change in frequency is quite simple, and it is straightforward to evaluate using the stiffness of the support system. With more than one support element, one would simply add the contributions from the elements, including rotational constraints as well. Comparing Equation 15 with 6, the result for the multi-DOF case reduces exactly to that of the single-DOF case, remembering that the mode shape has been mass normalized. Also note that the square of ω_p is in the denominator on the right-hand side of Equation 15. So at higher modal frequencies, $\Delta \omega_p / \omega_p$ varies proportionally as $(1/\omega_p)^2$.

We can now turn to the issue of damping in a supported structure. For the support damping, the situation is more complicated than for the modal frequency, because one will typically not have an analytical model of the damping in the structure. But the issue is the same as for the stiffness, given a measurement of the damping for a particular mode. How can we determine the change in the modal damping due to the support system? We will show in the following analysis that we can compute an approximation to the change in modal damping if the support system makes a negligible change

to the mode shape of the structure; and we have the mode shape components at the support connections and a damping model for the support system. Let us now look at the complex eigenvalue equation for a particular mode of the system:

$$\psi^T \left[K + i\omega_m \left(C_t + C_s \right) - \omega_m^2 M \right] \psi = 0 \tag{16}$$

where we have pre-multiplied by the transpose of that mode shape ψ. K is the total stiffness matrix, ω_m is the measured eigenvalue, i is $\sqrt{-1}$, C_t is the damping matrix for the true structure and C_s is that for the support structure. Now let us assume that the mode shape from the real eigenvalue problem can be used in Equation 16 to evaluate the damping in a mode. This basically assumes that the diagonal elements of $\psi' C \psi$ adequately reflect the damping in the system and that the off-diagonal terms can be ignored. Also implied in this assumption is that the mode shape changes negligibly with the addition of the support damping. The damping ratio is now defined conventionally as if the real modes did indeed diagonalize the damped system:

$$\zeta_m = \frac{1}{2\omega_m} \frac{\psi' \left(C_t + C_s \right) \psi}{\psi' M \psi} \tag{17}$$

Now we can define the true modal damping as before:

$$\zeta_t = \frac{1}{2\omega_t} \frac{\psi' C_t \psi}{\psi' M \psi} \tag{18}$$

Expand Equation 17 and combine with 18, taking the mode shape to be mass normalized, we have:

$$\zeta_m \omega_m = \zeta_t \omega_t + \frac{\psi' C_s \psi}{2} \tag{19}$$

which is very similar to Equation 7 derived for the single DOF system. Here the contribution due to the support damping has just been generalized to include the mode shapes. Solving for ζ_t, we find:

$$\zeta_t = \zeta_m \frac{\omega_m}{\omega_t} \left[1 - \frac{\psi' C_s \psi}{2\omega_m \zeta_m} \right] \tag{20}$$

This formula for the true damping ratio as the frequency formula, Equation 15, is a fairly simple expression. Given the measured modal damping, the measured modal frequency, the mode shape components at the support DOFs, and the damping model, the true damping ratio of the unsupported structure can be calculated. Equation 20 can also be compared to Eauation 8 for the single DOF case. Again, these equations are very similar, and Equation 20 reduces to Equation 8 for the single DOF case.

Equation 20 reveals some important features, just as Equation 8 did. Because the quantity in the brackets is the difference between one and a positive number, the difference between the true damping ratio and the measured damping ratio can be significant if the last term in the brackets is not close to zero.

Experimental Application – Uniform Beam

In this section, an experimental demonstration of these issues involving the support system is described. An extremely lightly damped system was chosen for the experiment to highlight the effects of the support system on the measured damping as well as measured frequency. To achieve the light damping, a 72-inch aluminum beam with a 1.0- by 1.5-inch cross-section was selected. The supports were placed at the ends of beam, the optimal locations for creating a change. Seven light-weight accelerometers were mounted at equal spacing on the beam to measure the mode shapes, although we were only interested in the first bending mode and the rigid-body bounce mode. The supports were very thin, long elastic cords attached at the ends; and the lengths of the cords were varied. Figure 3 shows a photo of the beam with its elastic supports.

The length of the elastic cords was varied with modal tests performed for eight different length configurations. Along with the first bending mode, the frequency and damping of the bounce mode were also measured for each configuration to ascertain the support stiffness and damping. Preliminary to these eight horizontally supported tests, one test was conducted with the beam

Figure 3. Photo of lightly damped aluminum beam with variable-length elastic supports.

$$\Delta \omega_p \cong \frac{1}{2\omega_p}\left(\phi_p^i\right)^2 \Delta k_{ii}$$

Figure 4. Comparison of the observed changes in modal frequency versus predicted changes using Equation (15).

Figure 5. Observed changes in modal damping as a function of the frequency ratio.

suspended vertically from a very long pendulum support at just one end. The pendulum frequency (lateral mode) was exceptionally low compared to the first bending mode to truly simulate a free support. This test condition was assumed to be the ideal condition from which all other test data would be compared. In this vertical suspension, the beam frequency was 58.6 Hz with 0.066 percent of critical damping. As mentioned earlier, the beam was very lightly damped, and the seven accelerometer cables actually did contribute to the nominal damping. Special care was taken so that the instrumentation cables and their lengths remained constant for all testing. The measured data from these nine tests are shown in Table 1, with the frequencies and dampings for the bounce mode and the first bending mode. The modal parameters were estimated using a frequency-domain, narrow-band algorithm. Included in the chart are the changes in the frequencies and dampings for each configuration as compared to the nominal data.

Examining the first column of the chart, one can see that the bounce frequency (support frequency) increased from 2.31 Hz to 8.65 Hz, so the frequency ratio decreased from 25 to 7. And we see an increase of 2.9 Hz (5 percent) in the frequency of the bending mode for the stiffest support condition. We can calculate the support stiffness because we have measured the bounce frequency, and along with the bending mode shape, we can apply Equation 15 to compute the predicted changes in measured frequency due to the support stiffnesses. Figure 4 plots the computed results versus the observed results as recorded in Table 1. The frequency changes are plotted as a function of the ratio of the elastic mode to the rigid-body bounce mode of the beam. As predicted from the theory, the change in the measured frequency diminishes as the ratio increases. Although here, one needs a ratio of approximately 15 before the frequency change drops below 1 percent. The predicted changes using Equation 15 follow the observed changes quite well. Recall that Equation 15 shows only the first-order effects, so there would be some differences. Equation 15 also assumes the support stiffness is not a function of frequency.

Figure 5 plots the change in the measured damping as a percent of the nominal damping versus the frequency ratio. Even for the highest frequency ratio of 25, there is a 100 percent change in the measured damping. In contrast to the changes in measured frequency, the measured damping for the bending mode has increased dramatically as the support has increased its stiffness and damping. For the worst case, the measured damping is 15 times that of the true damping (1400 percent increase). Of course, the
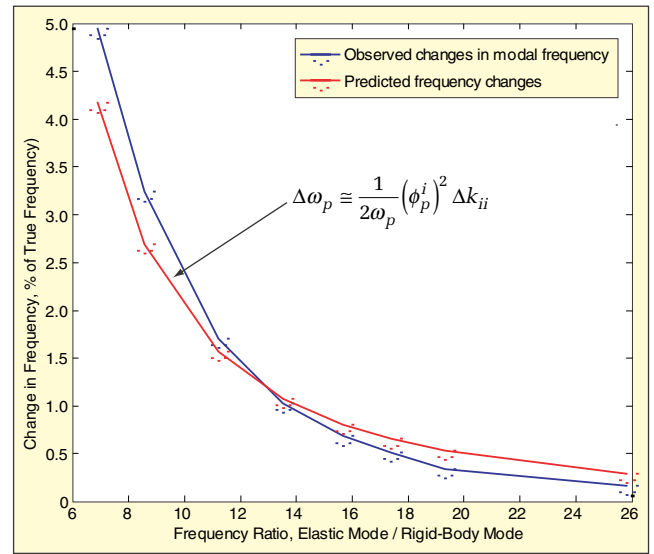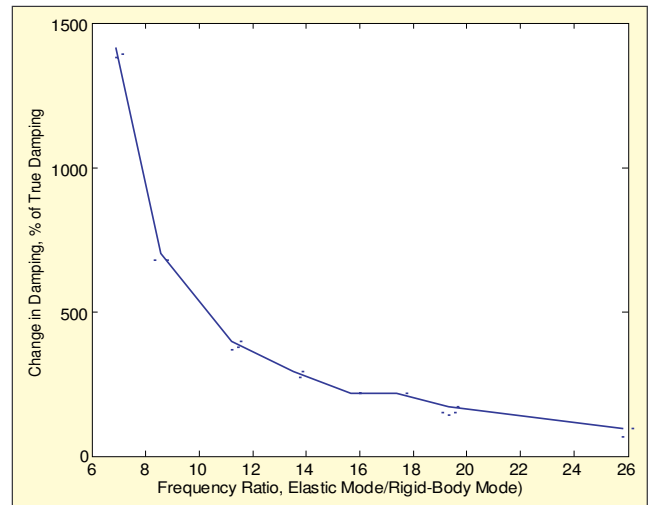
changes in damping have been intentionally amplified in this test because the beam structure was chosen to be very lightly damped. Nevertheless, these results do show how sensitive the measured damping can be to the support conditions. Even with supports designed using the rule of-thumb (frequency ratio = 10), the error in the measured damping can be huge.

One would like to contrast these observed changes in the measured modal damping to predicted changes using Equation 20. However upon application of Equation 20 using the viscous damping determined from the rigid-body modes, the predicted changes in damping vastly over-predicted the observed changes by factors of 5 to 10, convincing one that the viscous damping

Table 1. Measured frequency and damping data for the beam with variable support conditions.

Bounce Mode		First Bending Mode		Increase in Bending Frequency,		Increase in Bending Damping Factor	
Frequency, Hz	Damping Factor, % of critical	Frequency, Hz	Damping Factor, % of Critical	Hz	%	% of critical	% of damping
0.32 (pendulum)	~ 0	58.6	0.066				
2.31	3.7	58.7	0.13	0.1	0.2	0.06	90
3.09	4.3	58.8	0.18	0.2	0.4	0.11	170
3.43	4.5	58.9	0.21	0.3	0.6	0.14	220
3.81	4.3	59.0	0.21	0.4	0.8	0.14	220
4.41	6.7	59.2	0.26	0.6	1.0	0.19	300
5.31	8.6	59.6	0.33	1.0	1.7	0.26	400
6.96	11.7	60.5	0.53	1.9	3.1	0.46	700
8.65	13.2	61.5	1.00	2.9	5.0	0.93	1400

model was inappropriate for the supports. But upon application of Equation 11, the predicted changes were much smaller than those observed. Consequently, it is believed that the damping model for the supports should be a combination of both viscous and structural damping. Unfortunately, measurement of the damping at the rigid-body modal frequency does not provide sufficient data to fully characterize the support damping, so a comparison with predictions is not possible.

This test of a lightly damped uniform beam provides some interesting insights into support issues. It clearly shows the effect of the support stiffness on the measured modal frequency and the error that could result if one assumed the measured frequency was the true frequency. The formulas derived in the theory section adequately predict the observed changes in the measured frequency. For the measured damping, this example illustrates how very much the supports can affect the damping. Unfortunately, the damping changes could not be predicted because of an uncertain damping model. In the next section, we will examine modal test results from a production modal test of a wind turbine blade. Modal parameters were desired to validate the model both for stiffness and fatigue concerns, so the modal damping in the blade was required.

Experimental Application – Wind Turbine Blade

The tested wind turbine blade was the first blade of a series of new designs coming from the Sandia Blade System Design Studies (BSDS) program, and this blade was 27 feet long and weighed 290 pounds. This blade is from an exploratory development program and is much smaller than blades used for commercial turbines. A photo of the blade is shown in Figure 6. Additionally we note that the root end of the blade is 20 inches in diameter, and the blade CG location is nominally 84 inches from the root end. The blade was instrumented with 48 biaxial accelerometers plus 10 strain gauges in the flatback trailing edge region for a total of 106 measurement channels. The total mass of the instrumentation including the accelerometers, mounting blocks, and adhesive was 1.9 pounds. The blade was supported softly at two locations. Nylon straps were used to hold the blade using a choker style loop. The suspension was designed to be soft using bungee cords, as shown in Figure 6. A variety of bungee cord configurations were used for these tests, including a set of bungee cords deemed to be optimal.

The blade has two sets of bending modes, flatwise and edgewise. The flatwise modes involve bending about the x-axis (Figure 6) and bends the blade in its flat or soft direction. The edgewise modes involve bending about the y-axis or in the stiff direction of the blade. The flatwise bending modes are the lowest elastic modes of the blade, and consequently the support system was designed to
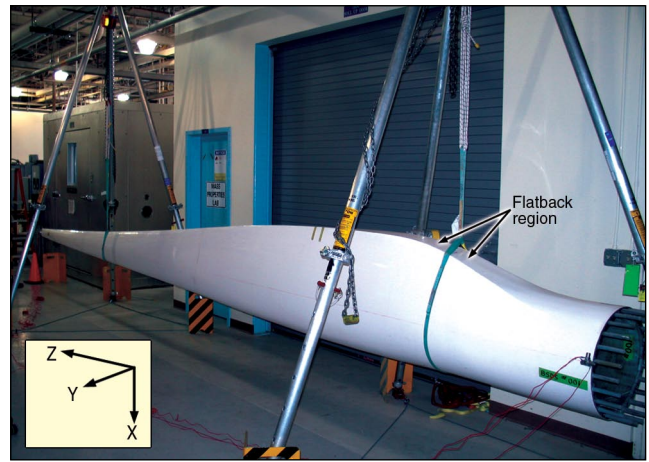
Figure 6. Photo of BSDS wind turbine blade in the test lab.

use the pendulum stiffness in the flatwise direction. The rigid-body pendulum modes are very low, and consequently have little effect on the measured frequencies. In contrast, the edgewise direction is directly restrained by the stiffness of the bungee cords, and their stiffness is enough to affect the measured modal parameters. Consequently we were mostly concerned with the effect of the support on the modal frequency and damping of the first edgewise bending mode, which is a bending mode in the direction of the bungees. Although for this particular blade structure, it was fairly easy to design a soft support system, because the blade had a high stiffness-to-weight ratio.

As part of the pre-test planning phase, bungee cords were tested for their stiffness and damping by suspending rigid masses from the bungee cords and measuring the resulting frequencies and damping factors. Their frequencies and damping factors were measured for various deformation amplitudes, frequencies of vibration and preloads on the bungee. Unfortunately, the stiffness and damping varied significantly with preload, amplitude and frequency, making it difficult to fully characterize the bungee cords and creating uncertainty in the bungee model. Consequently, after the pre-test design, the bungee cord characteristics were deduced from the rigid-body modal parameters measured during the actual test of the blade.

Four preliminary modal tests with very sparse instrumentation were conducted to experimentally assess the effects of various configurations of the support conditions. Table 2 describes these four configurations, designated 1, 2, 3, and 4.

For Configuration 1, the support is a stiff configuration with low load on each of the bungee loops. However, we found the rigid-body bounce mode at 4.7 Hz compared to the first edgewise bending at 16.38 Hz to be much too high, with a frequency ratio of only 3.4. For Configuration 2, we reduced the number of bungee loops from 8 to 6, and the bounce mode dropped from 4.7 to 3.2 Hz, producing a still high frequency ratio of 5.1, but the bending frequency decreased by 1.2 percent, and the damping factor went from 1.0 to 0.8 percent. Configuration 3, with the supports placed near the nodes of the mode, produced a total 1.8 percent reduction in frequency and a 27 percent reduction in damping even though the bounce mode increased in frequency. Configuration 3 clearly showed the advantage of placing the supports at the nodes of the affected mode, as Equation 15 implies. Configuration 4 is considered the optimal configuration, where the number of bungee

Table 2. Four different bungee configurations for supporting blade.

No.	Description	No. Loops	Motivation of Configuration
1 & 2	Bungees spaced 30 inches either side from CG	8,8	Low preload on each bungee loop of 20 lbs; safe support design
		6,6	Slightly higher preload (25 lbs) reduces stiffness of bungee loops
3 & 4	Near nodes of edgewise mode, 46 and 148 inches from CG	6,6	Moved to nodes of mode to reduce effect of bungee; preload changed
		4,2	Reduced number of bungees to reduce support stiffness and balance preload

Table 3. Measured modal parameters for four support configurations for bending and rigid-body modes.

	Rigid-Body Bounce Mode		First Edgewise Bending Mode				
Config.	Freq., Hz	Damping Factor, %	Freq., Hz	Increase from Config. 4, %	Damping Factor, %	Increase from Config. 4, %	Ratio of Edgewise to Bounce Freqs.
1	4.72	4.2	16.38	2.0	1.00	52	3.5
2	3.19	4.9	16.18	1.0	0.80	21	5.1
3	5.59	5.2	16.09	0.1	0.73	10	3.1
4	1.28	3.2	16.07	—	0.63	—	12.5

loops is further reduced to decrease the stiffness and placed on the nodes. The bounce frequency has now dropped to 1.28 Hz for a frequency ratio of 13. However, the frequency of the bending mode only decreased by 0.1 percent between Configurations 3 and 4, but its damping factor dropped from 0.73 to 0.63. These four support configurations demonstrate the effect that the support conditions can have on the measured modal parameters of the elastic modes, increasing the frequency by 2 percent and the damping by 59 percent. Even though this blade structure is quite stiff compared to its mass, it still requires careful consideration of the support design if one does not want to introduce significant errors to the measured modal parameters, particularly the measured modal damping. The measured frequencies and damping factors for these four configurations for both the rigid-body bounce mode and the first edgewise bending mode are listed in Table 3.

We can now compare the predictions using the developed formulas from the theory section with what we have observed from this test data. Comparing Configurations 1 and 4, we observed a frequency increase of 0.31 Hz and a damping factor increase of 0.37 percent of critical for Configuration 1. Using the rigid-body modal frequency and damping factor to compute the stiffness and damping of the bungee cords supporting the blade, we can predict the frequency change with Equation 15. Utilizing the mass normalized mode shapes from the pre-test analysis, we computed a predicted increase in frequency of 0.27 Hz, which is very comparable to the observed 0.31 Hz. Regarding the change in damping, we can also apply Equation 20, and here we compute that the true damping would be only 0.32 percent of critical. Actual damping for Configuration 4 is 0.63 percent. This clearly overestimates the effect of the support damping, which we would suspect is due to the fact that the damping model must include some structural damping as well as the viscous damping assumed in Equation 20. Using a structural damping model, we compute the true damping to be 0.80 percent, which underestimated the effects. So we are seeing the same results here as with the uniform beam. The viscous model overestimates, and the structural damping model underestimates the change in the measured damping. Nevertheless, this example from a production modal test on a wind turbine blade clearly illustrates the primary points of this article: support system stiffness can increase the measured frequencies above the true frequencies, and the measured damping is much more sensitive to the support system than the modal frequencies. Care must be exercised when designing a support system for 'free' modal tests.

Conclusions

In this article, we have examined the effects of support stiffness and damping on measured modal frequencies and damping ratios. The analysis of the single DOF system provided very revealing results that produced insight to the general system. The analysis of the multi-DOF systems produced results very similar to that of the single-DOF system, except now the mode shape of the elastic mode was included in the formulas. The increase in the measured frequency of the elastic mode was related to the square of the ratio of the frequencies of the rigid-body mode and the elastic mode. The damping was much more sensitive, since the damping in-

crease involved the ratio of frequencies rather than the square of their ratio and the ratio of the dampings. Consequently, even for a softly supported structure, the measured damping could be far from the true damping. These formulas can be used to aid in the design of a support system for modal testing of free or constrained structures.

The effects of the support system on both modal frequencies and modal damping were illustrated with two test structures. The first structure was an extremely lightly damped beam that revealed changes in the measured modal frequency and damping. The changes in the measured damping for the elastic mode were huge, indicating the care that musts be taken to accurately measure damping for a freely suspended structure. The second structure was a blade for a wind turbine in which modal data were required to validate the analytical model of the blade. Several support configurations were used for this blade, again revealing significant changes in the measured frequencies and dampings. These changes in the measured modal parameters were large enough that they needed to be taken into account to validate the blade model.

References
1. Bisplinghoff, R. L., Ashley, H., and Halfman, R. L., *Aeroelasticity*, Addison-Wesley Publishing Company, Inc., Cambridge, MA, pp. 771-779, 1955.
2. Strutt, J. W. (Lord Rayleigh), *The Theory of Sound*, vol.1, 2nd ed., Dover Publications, Inc., New York, 1945.
3. Wolf Jr., J. A., "The Influence of Mounting Stiffness on Frequencies Measured in a Vibration Test," SAE Paper 840480, Society of Automotive Engineers, Inc., 1984.
4. Carne, T. G., "Support Conditions, Their Effect on Measured Modal Parameters," Proceedings of the 16th International Modal Analysis Conference, SEM, pp 477-483.
5. Ewins, D. J., *Modal Testing: Theory, Practice and Application*, 2nd ed. Research Studies Press, Ltd, 2000.
6. Brillhart, R. and Hunt, D., "Part 1: The Pitfalls, Pratfalls, and Downfalls of Fixturing," *Experimental Techniques*, SEM, Vol. 29, No. 6, Nov/Dec, 2005, pp 58-61.
7. Avitabile, P., "Modal Space, Back to Basics," Experimental Techniques, SEM, Vol. 30, No. 3, May/June, 2006, pp 19-20.
8. Lazan, B. J., *Damping of Materials and Members in Structural Mechanics*, Pergamon Press, Elmsford, NY, 1968.
9. Slater, J. C., Belvin, W. K., and Inman, D. J., "A Survey of Modern Methods for Modeling Frequency Dependent Damping in Finite Element Models," Proceedings of the 11th International Modal Analysis Conference, SEM, pp 1508-1512.
10. Pilkey, D. F. and Inman, D. J., "A Survey of Damping Matrix Identification," Proceedings of the 16th International Modal Analysis Conference, SEM, pp 104-110.
11. Tsuei, Y. G. and Huang, B. K., "Effect of Modeling for Damping on Parameter Identification," Proceedings of the 16th International Modal Analysis Conference, SEM, pp 1427-1432.
12. Maia, N. M. M. and Silva, J. M. M., *Theoretical and Experimental Modal Analysis*, Research Studies Press, Ltd, 1997, p 32.

The author may be reached at: tgcarne@sandia.gov.